Algerian Journal of Research and Technology
ISSN : 2543-3954
A.J.R.T Volume 5 (N°1) (2021) 11 - 21

Optimizing the Performance of a Converter Dc/Dc in a Photovoltaic System

N. Mazouz*, A. Midoun

Laboratory of Power Systems and Solar Energy and Automatic (L.P.S.S.E.A), Faculty Electrical Engineering, Department of Electronics, University of Science and Technology of Oran. U.S.T.O.M.B, PO. Box 1505 El M'naouer USTO, Oran, Algeria

* *Corresponding author:* mazouz.usto@gmail.com, nacera.mazouz@univ-usto.dz

Received 29 January 2019; Accepted 06 May 2019

Abstract. The objective of this scientific research is the development of DC / DC converters for optimizing the efficiency of a photovoltaic system, as to find the most accurate mathematical modeling possible to predict behavior, and to provide Measurable information related to the physical quantities of the system.
The search for the maximum power point is the essential work in the optimization of photovoltaic systems because there is a problem of adaptation between the load characteristics and the maximum power point of the photovoltaic generator. The optimization deals with the electrical operating parameters of the solar generator.
A photovoltaic generator can operate in a wide range of voltage and output current but it can deliver maximum power only for particular values of current and voltage. , thus the realization of an experimental prototype for the characterization of the converter using different control techniques VMC (Voltage Mode Control) and PCM (Peak Current Mode).

Keywords. DFT, Half-metallic ferromagnetic, Co-doped 4H-GaN polytype, BoltzTrap.

INTRODUCTION

However, one of the major problems with the widespread use of renewable energy is to further reduce the cost of systems while increasing their costs. Yield but if the first challenge is the manufacturing technology there is another problem that concerns the systems of adaptation of this energy for its exploitation in different applications such as the pumping of water, the control of the electric motors, the lighting, battery charging, satellite power supply etc. The DC / DC converter in photovoltaic systems is subject to a disruptive environment, imprecise and uncertain variation of climate parameters and sensitivity to intrinsic parameter variation of GPV (manufacturing technology), which may affect the operation and performance of performance of the DC / DC converters as well as the load connected to its output. The analysis of the dynamic behavior of the converter is based on the SSA (State Space Averaging) method. The interaction with the load and the source is analyzed with respect to the impedance of the converter. Practically it is very difficult to measure and control these quantities, it is for this reason that it is recommended to design an optimal converter based on regulator where the load and the source does not affect the performance of the DC-DC converter.

STRUCTURE OF THE DEVELOPED SET UP

The prototype consists of a Superbuck converter representing the power board and a control board based on a microcontroller Microchip family (Figure 1). Both control techniques and the control loop were implemented separately in order to facilitate the characterization of the converter. A PID controller was designed to test the stability and performance of our Superbuck converter (Mazouz, 2014).

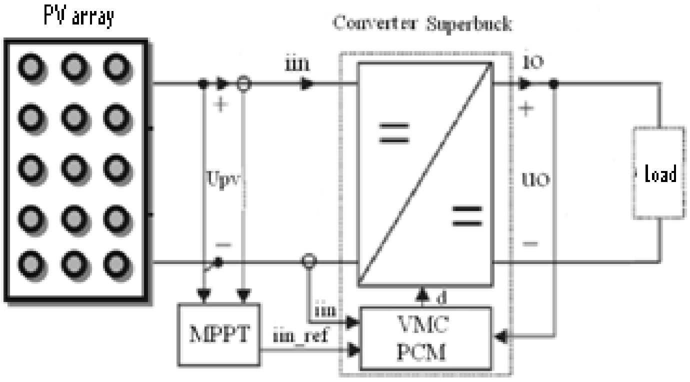

Fig. 1. Block diagram of the converter closed loop.

Table 1. Values of the components used for the study of Superbuck converter.

Voltage source	Uin =20V	
Voltage across the load	Uo =10 V	
Current load	Io =2.5 A	
Inductors	L_1=15 µH;	r_{L1}=5 mΩ
	L_2=15,2 µH;	r_{L2}=5mΩ
Capacitors	C_1=20 µF;	r_{C1}=0.7 mΩ
	C_2=25 µF;	r_{C2}=0.7 mΩ
Diode	U_D=0.3 V;	r_d=50mΩ
load On in the MOSFET	r_{ds} =0.25Ω	
Switching frequency	f_s=5KHz	Ts=1/f_s=200µs
Load Resistance	R_L=8 Ω	

CONTROL STRATEGIES

Voltage Mode Control VMC

The dynamic model of Superbuck TLC controlled mode VMC shown in figure 2 (Karppanen et al., 2007; Suntio, 2009).

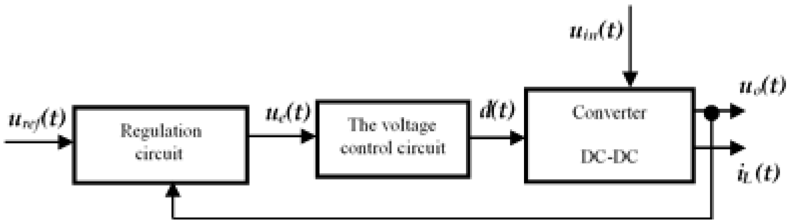

Fig. 2. Voltage Mode Control VMC.

Current Mode Control CMC

Among the techniques of CMC command mode, that the PCM is of most interest to control the converter as long as it allows continuous control of the current, it is very often the one chosen for the switch. The error signal is generated by the difference of the output voltage $u_o(t)$ at a reference u_{ref} ; a current $i_{co}(t)$ is obtained following the application of the error signal to a control circuit (Figure 3) (Karppanen et al., 2007; Suntio, 2009).

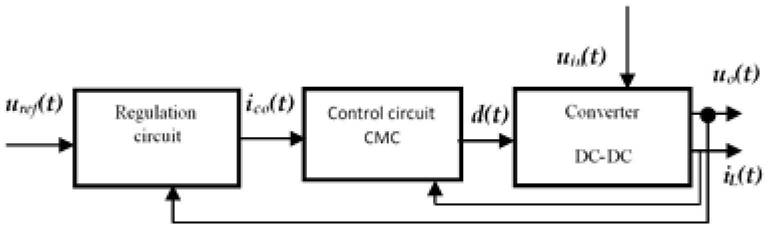

Fig. 3. Current Mode Control CMC.

PV Performance Optimization

The search for the maximum power point is the essential work in the optimization of photovoltaic systems because there is a problem of adaptation between the characteristics of charge and the maximum power point of the PV array. These converters, known as MPPT (Maximum Power Point Tracking) see figure 4, coupling between the PV generator and the receiver forcing the first to deliver maximum power.

The objective of this study is to highlight the transients caused by the order first, and disruptions in the PV generator and the other receiver. The study of the stability of the system used to define the permissible range of the order and the ideal dynamic behavior.

The principle of this control (MPPT) extremely is very simple. Starting from a command with a small duty cycle (and thus large VPV) increases d regularly. Initially the power increases (the maximum is not reached 1) stabilizes (the maximum is reached then 2) and decreases (the maximum has been exceeded 3). The measuring system detects this reduction in power, which determines a reversal of the order: the power will then increase, go through the maximum and then decrease; early detection of this decrease in power, the sense of the order is reversed again. Finally, the system goes into oscillation around the maximum (Mazouz, 2014).

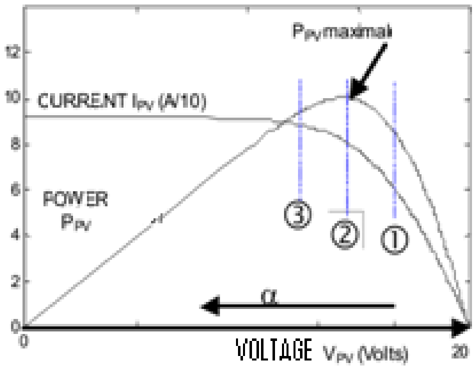

Fig. 4. Variationof the duty cycleinfunctionofthe characteristic I-V and P-V.

Modeling of DC-DC converters

It is important to have a powerful mathematical model of the converter to improve and facilitate in particular its design and production spot, is the attraction most important and fundamental responsibility of the designer. This modeling is done in two stages: study static and dynamic study (Karppanen et al., 2007).

The signals shown in figure 5 are respectively: input voltage (u_{in}), output voltage (u_o), input current (i_{in}), output current (i_o) and duty cycle (d).

The static model is determined when the converter is in continuous operation where all variables remain constant, or that there are always fluctuations, different backgrounds around each size as shown in figure 5, these fluctuations are often neglected when trying to determine the converter resting point to ensure its operation around that point.

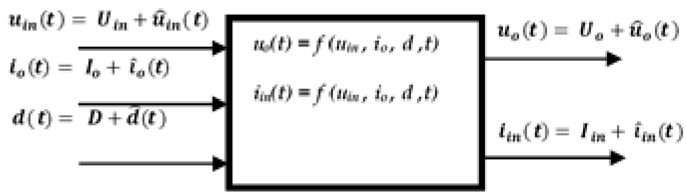

Fig. 5. Block diagram of input and output signals of the converter.

As part of a dynamic study, the behavior of the converter is not the same as steady as we consider only static variables, or in this case, each variable (DC or AC) has its effect on response of the converter.

For representation in the state space of the form (Suntio, 2009):

$$\begin{cases} \frac{d\hat{x}}{dt} = A\hat{x}(t) + B\hat{u}(t) \\ \hat{y}(t) = C\hat{x}(t) + D\hat{u}(t) \end{cases} \quad (1)$$

Laplace transform of the system:

$$\begin{cases} X(s) = C(sI - A)^{-1} BU(s) \\ Y(s) = C\,X(s) + E\,U(s) \end{cases} \quad (2)$$

$\Rightarrow Y(s) = H(s)U(s)$ (3)

Such as : $H = C(sI - A)^{-1}\,B + E$ (4)

Thus, the various transfer functions are such that:

$$\Leftrightarrow \begin{bmatrix} \hat{\imath}_{in} \\ \hat{u}_o \end{bmatrix} = \begin{bmatrix} Y_{in-o} & T_{ji-o} & G_{ci} \\ G_{io-o} & -Z_{o-o} & G_{co} \end{bmatrix} \begin{bmatrix} \hat{u}_{in} \\ \hat{\imath}_o \\ \hat{c} \end{bmatrix} \quad (5)$$

Where the matrix H(s) was formed by:
Y_{in-o} : the input admittance converter;
T_{ji-o} : the inverse transform of the output-input transfer function;
G_{ci} : control-input transfer function;
G_{io-o} : input-output transfer function;
Z_{o-o} : the output impedance of the converter;
G_{co} : control-output transfer function;
C: the command of duty cycle (d)
The index ‘’o’’ means: open loop.
Equation (5) describes "the model converter small signals in the frequency domain operating in open loop" (Figure 6).

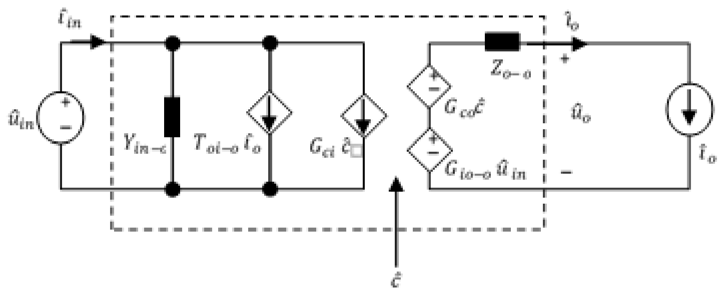

Fig. 6. The Small signal dynamic model of a DC-DC converter.

Regulator design

The choice of regulator is based on the analysis previously made on the system, in particular on the command-output transfer function $\boldsymbol{G_{co}}$, which contributes directly in $\boldsymbol{L_u(s)}$.
To develop the correct regulator for our system, we will apply the method, which consists in analyzing its response (the Bode diagram) in order to choose the type and the parameters of the regulator.
Figure 7 illustrates the form of the uncompensated $L_u(s)$ function (without regulation) defined by equation (6).

$$L_u(s) = G_{se}\, G_a\, G_{co} \quad (6)$$

Such as :

$$G_{co}(s) = \left. \frac{\hat{u}_o(s)}{\hat{\imath}_{co}(s)} \right|_{\hat{u}_{in}(s)=\hat{\imath}_o(t)=0}$$

$$\boldsymbol{G_a} = 1$$

$$\boldsymbol{G_{se}} = \frac{1}{R_s}$$

$\boldsymbol{G_{se}}$: Gain of the output voltage sensor;
$\boldsymbol{G_a}$: Modulation circuit gain;
$\boldsymbol{G_{co}}$: control-output transfer function of the Superbuck converter.

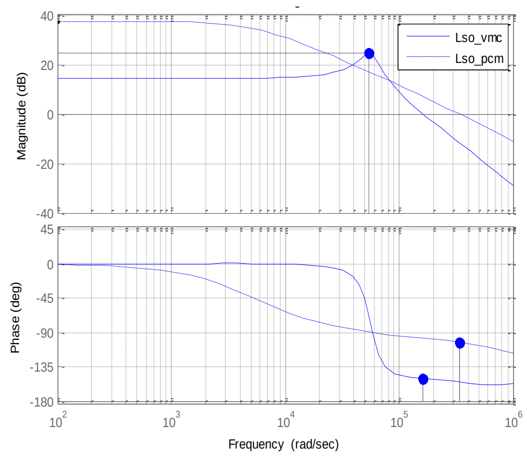

Fig. 7. Frequency response of the L (s) function without Lu(s) regulation.

Analysis of the Bode diagram shows that the system is characterized by a cutoff frequency of $\boldsymbol{f_c}$= 59.7 kHz, a phase margin of PM = 79.8 ° and absence of GM gain margin; RHP-z limits system bandwidth; therefore the choice of cutoff frequency should be lower than that of RHP-z in order to escape its effect.
Therefore, this system is stable but its robustness is not guaranteed and its bandwidth is too narrow, slower system.
The objective is to improve these parameters (PM and GM) to make the system more robust to possible disturbances. Under this pretext, we will seek to design a regulator which allows us to satisfy our conditions, improvement of the bandwidth, a phase margin belonging to [45°, 60°], and a gain margin of between 8 and 15 dB.
Under this pretext, a PD compensator (phase advance compensator) and a PI compensator (phase delay compensator) are introduced into the system in order to obtain the desired phase and gain margin.
The study closed loop shows that the converter input impedance Z_{in_c} is low at low frequencies in VMC and PCM controls the two techniques in a similar way and that for both types of linear source and PV, this attenuation is due to the reaction against the output current to a 90 ° phase shift for VMC control. By cons, at high frequencies the input impedance remains magnitude that justifies the stability of the operating point of the converter figures (8,9) (Mazouz, 2014).

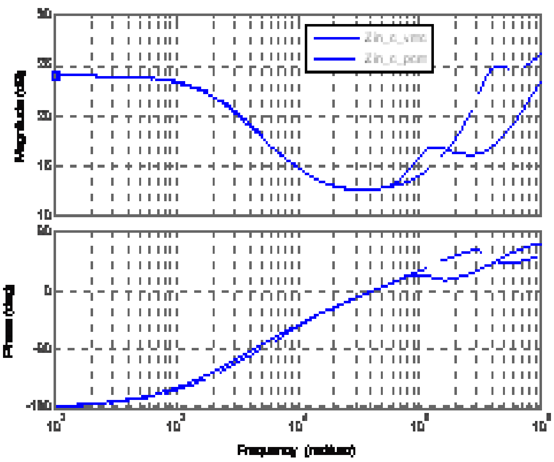

Fig. 8. Closed loop frequency representation in the input impedance Zin_c connected to a source Fixed.

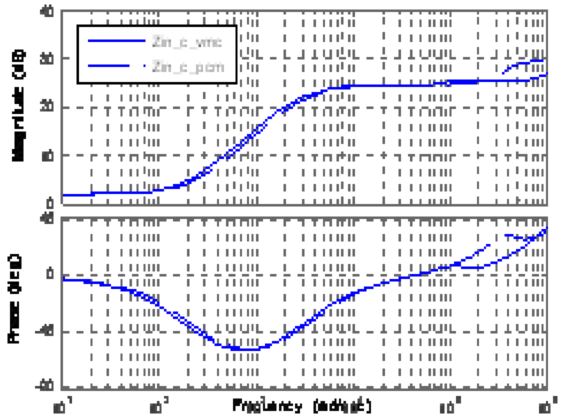

Fig. 9. Closed loop frequency representation in the input impedance Zin_c connected to a PV source.

Effect of the ratio on the step response transfer function G_{io}

The G_{io}feature to determine the influence of harmonic $\hat{u}_{in}$ entries on the output voltage $u_0(t)$ of the converter, so it defines how changes or disturbances introduced on the input voltage $\hat{u}_{in}$ result at $\hat{u}_0$ (equation 7)

If: $G_{io-o} = 0$,$\hat{u}_0$=-$Z_{-oo}\hat{i}o \quad + G_{co}\hat{d}$ (7)

Having said that the output dynamic range is completely immunized against the source effect. The figures (10, 11,12) show the influence of duty cycle d of the output. The more one evolves duty cycle, the greater the output dynamics are stable.

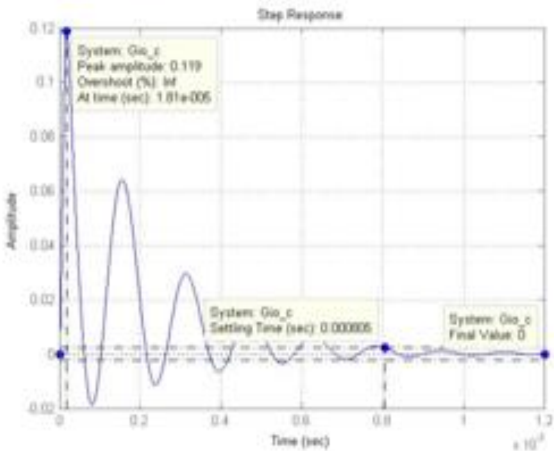

Fig. 10. The step response transfer function G_{io}, $d = 20\%$.

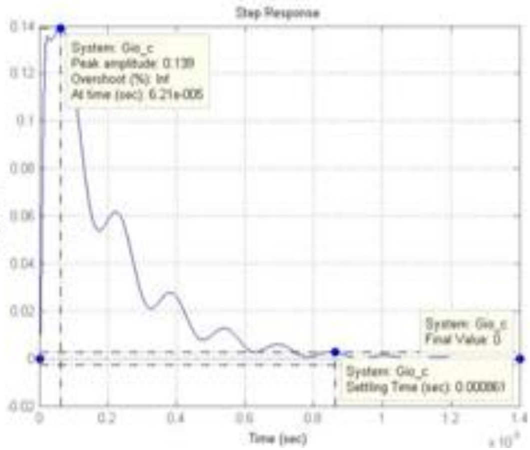

Fig. 11. The step response transfer function G_{io}, $d = 60\%$.

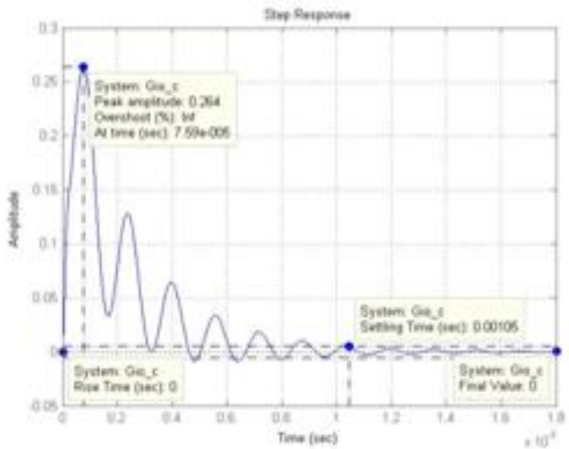

Fig. 12. The step response transfer function G_{io}, $d = 90\%$.

Practical realization of the prototype

Realized converter consists of a transistor MOSFET IRF740, BY30F diode, two capacitors and two inductors with the values given in Table 1. The MOSFET transistor is used as switching element because of its ease of control, high efficiency and rapid switching. In addition, the power diode that can withstand the extreme peak coil current is used (figure 13, 14). Both commands techniques as well as the control loop have been implemented separately in order to facilitate the characterization of the converter and this by using a type 18F452 microcontroller. The digital control has been selected for the closed loop operation, where the two techniques have been implemented in the microcontroller, the control of the output voltage will be held. A PID controller was designed to test the stability and performance of our Superbuck converter. The 18F452 microcontroller is used to perform this task; it contains an analog / digital converter, a pulse generator and especially a high clock frequency. To test the performance of our control, resistive load were used at the output from the converter (Mazouz, 2014).

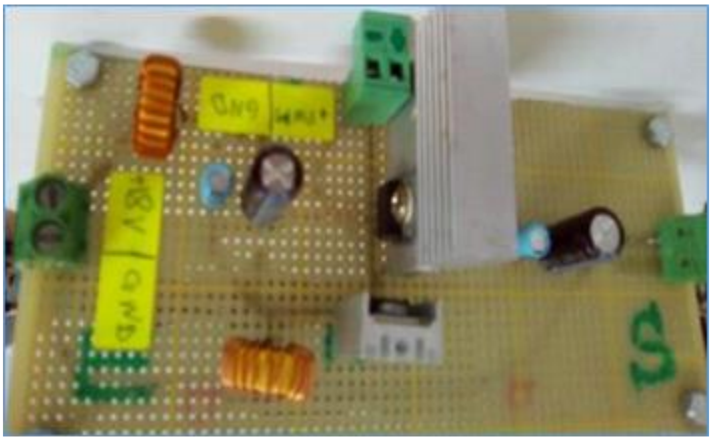

Fig. 13. Superbuck converter test bench.

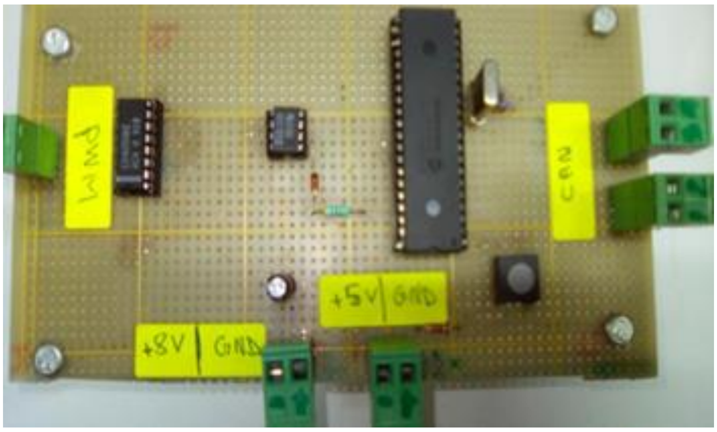

Fig. 14. Maximum Power Point Tracker MPPT test bench.

To test the operation of our converter, we took samples of the output voltage, the output current and the control pulses for both VMC and PCM techniques. The figures (15, 16) show the output voltage in VMC mode and the MPPT control with the Superbuck converter.
In order to test the functioning of our converter, we took samples of the output voltage, the output current as well as the control pulses for the two techniques VMC and PCM.

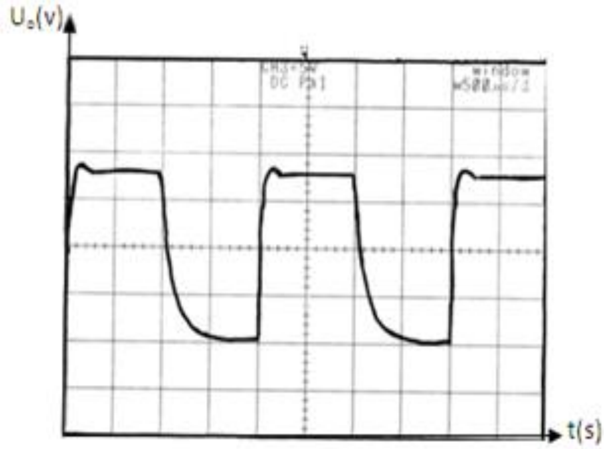

Fig. 15. The output voltage of the MPPT controlled Superbuck converter.

Fig. 16. The output voltage of the Superbuck controlled converter VMC driven by a photovoltaic source.

Figures 17 and 18 shows the output voltage, the output current and the pulses for the two commands VMC, PCM respectively with a switching frequency of 5 KHz.
The measurements carried out practically in VMC and PCM mode, with those of the simulation show that the results are similar with a certain tolerance, which is due to the delay imposed by the control chain (the driver, the transistor, etc.).

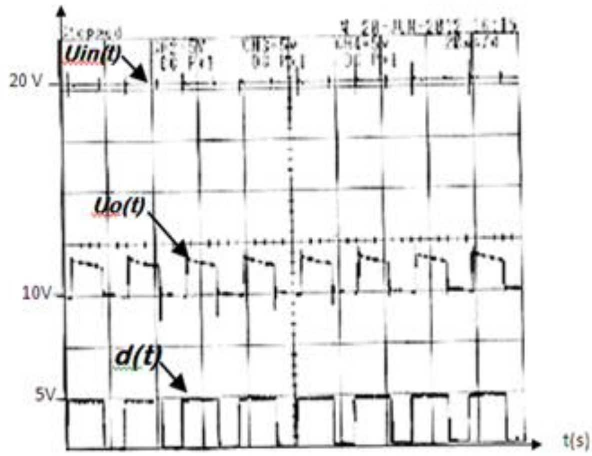

Fig. 17. Superbuck converter operation in PCM mode the input voltage, the output voltage, the control signal d.

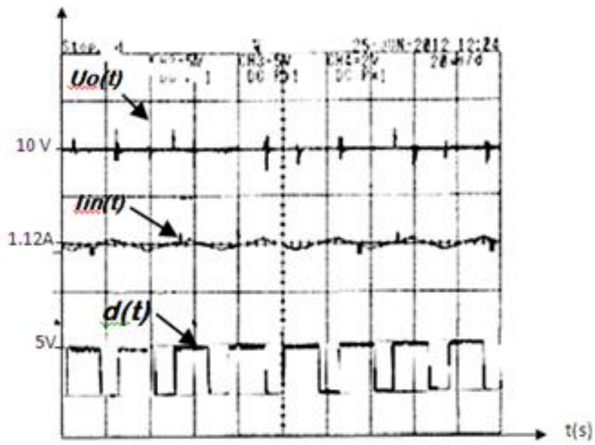

Fig. 18. Superbuck converter operation in PCM mode the output voltage, the input current, the control signal d.

CONCLUSION

The results obtained proved that the found mathematical models give a good prediction on the dynamic behavior of the Superbuck converter for the two types of fixed and photovoltaic sources used. In addition, the study done for a photovoltaic source definitively proves that the operating margin of a Superbuck converter can cover the entire curve of the operating points of the PV generator without observed constraints. Limiting the output voltage may, however, make the converter unstable at the peak power point PPM.

In conclusion, the dynamics of a DC / DC converter does not only depend on its topology but also on the control technique. The prospects are to be able to apply the two VMC and PCM commands on other static converters in order to benefit from their advantages and overcome problems often encountered when analyzing power systems.

The results obtained by simulation have shown that the impedance in VMC mode does not equal to zero therefore the interaction can be amplified with the source and the load, On the other hand in PCM mode, the only drawback of this control technique c 'is the output impedance is important therefore the Superbuck converter is affected by load impedance.

REFERENCES

Karppanen M., Suntio T., Sippola M., 2007. IEEE Transactions on Industrial Electronics. 54 (2).

Mazouz N., 2014. PhD Thesis. Electrical Engineering Faculty, Institute of Electronics, USTO, Oran, Algeria; 2014.

Teuvo S., 2009. Analysis And Control”.1stEdition WILEY-VCH.